Optoelectrofluidic behavior of metal–polymer hybrid colloidal particles

Dongsik Han, Hyundoo Hwang, and Je-Kyun Park

Related Articles

Modeling the motion and detection of particles in microcantilever sensor cells
J. Appl. Phys. 113, 114501 (2013)

Sub-picowatt resolution calorimetry with a bi-material microcantilever sensor
Appl. Phys. Lett. 102, 103112 (2013)

Review article: Fabrication of nanofluidic devices
Biomicrofluidics 7, 026501 (2013)

An active one-particle microrheometer: Incorporating magnetic tweezers to total internal reflection microscopy
Rev. Sci. Instrum. 84, 033702 (2013)

A negative-pressure-driven microfluidic chip for the rapid detection of a bladder cancer biomarker in urine using bead-based enzyme-linked immunosorbent assay
Biomicrofluidics 7, 024103 (2013)

Additional information on Appl. Phys. Lett.

Optoelectrofluidic behavior of metal–polymer hybrid colloidal particles

Dongsik Han,[a] Hyundoo Hwang,[a] and Je-Kyun Park[b]

Department of Bio and Brain Engineering, Korea Advanced Institute of Science and Technology (KAIST),
291 Daehak-ro, Yuseong-gu, Daejeon 305-701, Republic of Korea

Behavior of metal–polymer hybrid colloidal particles in an optoelectrofluidic device has been investigated theoretically and experimentally. In the application of hundreds of kHz ac voltage, a variety of optically induced electrokinetic and electrostatic mechanisms affect the movement of gold-coated polystyrene microspheres. The particles repel from the light pattern, and their mobility increases as the amount of gold increases. We apply this model to develop an optoelectrofluidic immunoassay, in which the corresponding metal–polymer hybrid particles are formed by a reaction of antibody-coated gold nanoparticles, antigens, and antibody-coated polystyrene microspheres. © 2013 American Institute of Physics. [http://dx.doi.org/10.1063/1.4790622]

Optoelectrofluidics refers to the study of motion of particles and fluids under an electric field induced or perturbed by an optical field.[1] Among several types of optoelectrofluidic technologies, optoelectronic tweezers (OET),[2] which is based on optical-to-electrical energy transfer process via a photoconductive layer, has come into the spotlight as a powerful technology for programmable optical manipulation. The OET has been applied not only for manipulation of biological materials such as blood cells,[3] oocytes,[4] sperms,[5] ciliates,[6] and biomolecules[7] but also for analytical applications, including molecular diffusion measurement,[8] sandwich immunoassays,[9] and a surface-enhanced Raman scattering-based molecular detection.[10] In addition, a variety of physical phenomena occurred in the OET device have also been heavily studied.[11–14]

Hybrid colloidal particles have unique properties that cannot be found in homogeneous materials. For instance, metal–polymer hybrid colloidal particles could be utilized in electronic[15] and photonic[16] applications due to the conductivity and permittivity of their metallic composition without losing intrinsic advantages of polymer particles such as versatility and easiness in manipulation and modification. These unique properties have led the metal–polymer hybrid colloidal particles to be studied actively in recent years. For example, they could perform a role to detect analytes spectroscopically, particularly in immunoassays by coating with metallic materials.[17] Besides, optically encoded microparticles, which can be used in multi-colored assays such as DNA hybridization study, were developed by linking quantum dots.[18] Metal–silica hybrid nanostructures for surface-enhanced Raman spectroscopy are also demonstrated, and each structure can be yielded as a hybrid particle.[19] To investigate physical characteristics in electric field, dielectric properties of a metal–polymer hybrid particle have also been studied.[20]

In this letter, we describe a behavior of metal–polymer hybrid colloidal particles in an optoelectrofluidic system, where a variety of optically-induced electrokinetic and electrostatic forces act on the particle movements in concert. We also propose an immunoassay platform based on the change in optoelectrofluidic motility of immunocomplexes, which are metal–polymer colloidal particles composed of polystyrene (PS) microspheres and gold nanoparticles (AuNPs) with target antigens.

The optoelectrofluidic device, which consists of two parallel plates, is schematically presented in Fig. 1(a). The upper plate is a glass substrate coated with indium tin oxide (ITO), and the bottom plate is a photoconductive layer-coated ITO–glass substrate. The photoconductive layer in the bottom plate was fabricated by sequential deposition of three layers: (1) a 50 nm-thick heavily doped hydrogenated amorphous silicon (a-Si:H); (2) an 1 μm-thick intrinsic a-Si:H, and (3) a 20 nm-thick silicon nitride on the ITO-coated glass substrate using a plasma enhanced chemical vapor deposition method. An 1 μl of sample droplet containing colloidal particles was placed in an 80 μm-height liquid chamber between those two plates,
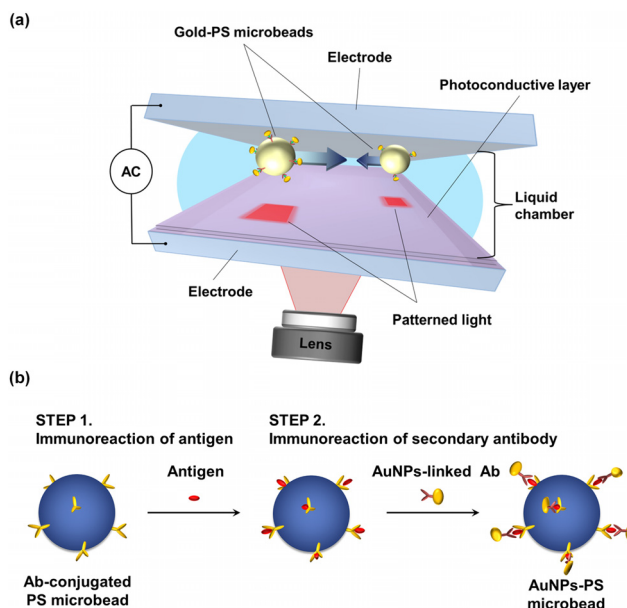

FIG. 1. Schematic illustration of (a) the optoelectrofluidic device and (b) synthesis of a AuNPs–PS hybrid particle. The hybrid particles were formed via immunoreaction of antibody (Ab)-conjugated AuNPs, antigens, and Ab-conjugated PS microbeads.

[a]D. Han and H. Hwang contributed equally to this work.
[b]Electronic mail: jekyun@kaist.ac.kr. Tel.: +82-42-350-4315. Fax: +82-42-350-4310.

and then an ac voltage of 20 $V_{peak-peak}$ with 100 kHz was applied across the ITO electrodes. When a light pattern produced by a liquid crystal display was projected onto the photoconductive layer, only the illuminated area became conductive, resulting in a nonuniform electric field in the liquid chamber. As a consequence, metal–polymer hybrid particles in the sample droplet were forced to move via optically induced electrokinetic mechanisms. In this study, gold-linked PS particles were used as the metal–polymer hybrid particles. They were synthesized by immunoreaction of 6 μm carboxylated PS microbeads (Polysciences, Inc., Warrington, PA) conjugated with goat anti-mouse IgG (Sigma–Aldrich, St. Louis, MO), normal mouse IgG, and goat anti-mouse IgG-conjugated AuNPs (5 nm in diameter; Sigma–Aldrich), as shown in Fig. 1(b). To conjugate the anti-IgGs to the microbeads, a general conjugation chemistry based on 1-ethyl-3(3-dimethylamino-propyl)cabodiimide (EDC) plus sulfo-N-hydroxysuccinimide (sulfo-NHS) was used.[21] First, 30 μl of carboxylated PS microbeads (2.10 × 10^8 microbeads/ml) were transferred to the microcentrifuge tube. Microbeads were washed by centrifugation with deionized water at 10 000 g for 5 min three times and resuspended in 300 μl of 0.1 M 2-(N-morpholino)ethanesulfonic acid buffer (pH 6.0). To activate microbeads, 100 μl of 460 mM sulfo-NHS and 100 μl of 156 mM EDC were added to a solution containing microbeads and incubated for 30 min at room temperature. The resulting microbeads were collected by centrifugation at 10 000 g for 3 min at 4 °C, and the supernatant was carefully discarded. The microbeads were resuspended in 100 μl of 0.15 M phosphate buffered saline (PBS) buffer (pH 7.2), and the activated microbeads were incubated with anti-IgGs for overnight in an automated mixer. The conjugated microbeads were finally washed three times with PBS buffer and resuspended in 500 μl of the same buffer. 3 μl of antibody-conjugated microbeads solutions were resuspended in 37 μl PBS buffer and reacted with 20 μl of serial diluted antigen solutions and 10 μl of AuNP-linked secondary antibody solutions for 10 min at room temperature in series. After incubation, AuNP-linked PS microbeads were collected by filtering and resuspended in 50 μl of deionized water.

When a light pattern was projected onto the photoconductive layer, the metal–polymer hybrid particles were focused toward the upper electrode and moved away in a lateral direction from the light, which forms the virtual electrode [Fig. 2(a)]. Here, the changes in the vertical position of the particles could be observed using a microscope with a lens having a relatively short depth of focus. The hybrid particle in the upper image was synthesized by immunoreaction with 0.1 ng/ml IgG solution, and the bottom one was synthesized with 1000 ng/ml IgG solution, which means the bottom one has relatively large amounts of AuNPs on the PS particle surface. The two metal–polymer hybrid particles both moved away from the light pattern in a lateral direction but showed different optoelectrofluidic mobility depending on the amount of AuNPs they have. The AuNPs–PS hybrid particles with relatively large amounts of AuNPs moved with higher velocity than the hybrid particles linked with small amounts of AuNPs. It is no wonder that the electrokinetic behavior of the hybrid particles varies according to the amount of AuNPs, which dominantly affects the electrical properties of the hybrid particles. Then, what phenomena are the causes of this behavior
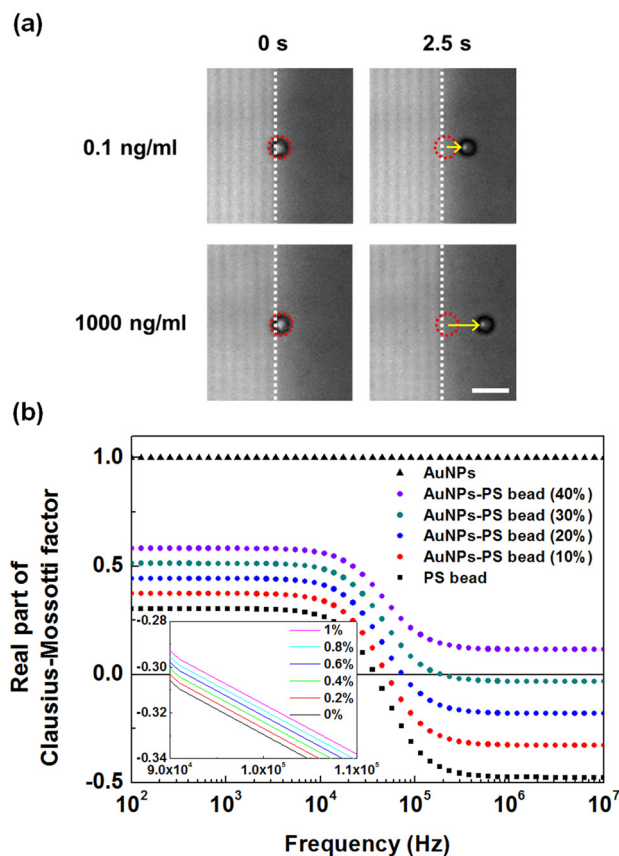

FIG. 2. (a) Microscopic images showing the motion of hybrid particles according to antigen concentration (0.1 and 1000 ng/ml) in the application of an ac voltage of 20 $V_{peak-peak}$ with 100 kHz (scale bar: 10 μm). White portions are optically generated virtual electrodes. (b) Theoretically calculated real part of CM factor for a AuNPs–PS hybrid particle against the fraction of the gold-coated area in the hybrid particle surface. The real part of CM factor increases in positive direction as the fraction of gold-coated area increases from 0% to 40%. The inset graph shows the CM factor variation near 100 kHz according to the fraction of gold-coated area from 0% to 1%. Both graphs have the same unit.

difference according to the amount of metal particles? The dielectrophoretic force acting on a particle is defined as $F_{DEP} = 2\pi r^3 \varepsilon_m \mathrm{Re}[f_{CM}]\nabla E^2$, where r is the radius of the particles, $\varepsilon_m = \varepsilon_0\varepsilon_r$ is the permittivity of the suspending medium, where ε_r is the relative permittivity of the fluid and ε_0 is the permittivity of free space, $\mathrm{Re}[f_{CM}]$ is the real part of the Clausius–Mossotti (CM) factor, and E is the local electric field. $\mathrm{Re}[f_{CM}]$ of the metal–polymer hybrid particle can be expressed as the proportional sum of those of homogeneous polymer and metal-coated polymer as below

$$\mathrm{Re}[f_{CM,metal-polymer\ hybrid\ particle}] = (1-m) \cdot \mathrm{Re}[f_{CM,polymer}] + m \cdot \mathrm{Re}[f_{CM,metal-coated\ polymer}],$$

where m is the metal-occupied ratio on the surface of metal–polymer hybrid particle.[22] The CM factor of homogeneous polymer is described as

$$f_{CM,\ polymer} = \frac{(\varepsilon_p^* - \varepsilon_m^*)}{(\varepsilon_p^* + 2\varepsilon_m^*)},$$

where ε_p^* and ε_m^* are the complex permittivities of the polymer particle and medium, respectively; $\varepsilon^* = \varepsilon - (\sigma/\omega)\,\mathrm{j}$, where σ

is the conductivity, ε is the permittivity, and ω is the angular frequency. Meanwhile, we applied a spherical shell model to calculate the CM factor of metal-coated polymer particles. According to the shell model, the CM factor of the metal-coated polymer is described as

$$f_{\text{CM, metal-coated polymer}} = \frac{(\varepsilon_{\text{mp}}^* - \varepsilon_{\text{m}}^*)}{(\varepsilon_{\text{mp}}^* + 2\varepsilon_{\text{m}}^*)}.$$

Here, the metal-coated polymer particle complex permittivity $\varepsilon_{\text{mp}}^*$ is given by $\varepsilon_{\text{mp}}^* = \varepsilon_{\text{metal}}^*[\gamma^3 + 2(\varepsilon_{\text{p}}^* - \varepsilon_{\text{metal}}^*)/(\varepsilon_{\text{p}}^* + 2\varepsilon_{\text{metal}}^*)]/[\gamma^3 - (\varepsilon_{\text{p}}^* - \varepsilon_{\text{metal}}^*)/(\varepsilon_{\text{p}}^* + 2\varepsilon_{\text{metal}}^*)]$ where the factor γ is the radius ratio of a metal-coated polymer particle to a polymer particle.[23] As a result, Re[$f_{\text{CM, metal-polymer hybrid particle}}$] of the AuNP–PS hybrid particles that we used in this study could be calculated against the amount of AuNPs on the PS particle surface [Fig. 2(b)]. The assumed relative permittivities of PS bead, AuNP, and medium that we used for simulation are 2.55, 6.9, and 78, and their conductivities are 2.3×10^{-4}, 4.5×10^{7}, and 0.5×10^{-4} S/m, respectively. At a frequency of 100 kHz, Re[$f_{\text{CM, metal-polymer hybrid particle}}$] increases from negative value to positive value as the concentration of AuNP–PS hybrid particles increases. This means that repulsion force by dielectrophoresis (DEP) decreases as the concentration of AuNP–PS hybrid particles increases. Although the hybrid particles having small amounts of AuNPs should be more rapidly repelled from the light pattern according to the calculation, our experimental results showed a totally different tendency [Fig. 2(a)]. In other words, the particle behaviors observed in this study are inexplicable based on the conventional theories, in which optically induced DEP plays the most dominant role on the particle behaviors in the optoelectrofluidic devices in the application of hundreds of kHz ac voltage.[14,24]

To account for the behavior of particles, here we have two more mechanisms which should be occurred in the opto-electrofluidic device as dominant as the optically induced dielectrophoretic force. One is the ac electro-osmosis (ACEO) flow, which is caused by the motion of ions along the surface of electrode by a tangential electric field, can be defined as $\langle v_{\text{slip}}\rangle = -\lambda_{\text{D}}\text{Re}[\sigma_{\text{q}}E_{\text{t}}^*]/2\eta$, where λ_{D} is the Debye length, σ_{q} is the charges contained in the electric double layer, E_{t} is tangential electric field, and η is the fluid viscosity [see Fig. S1 in supplementary material[25]]. The other is the electrostatic interaction between the particle and the electrode surface, which is determined by $F_{\text{electrostatic}} = (-3\pi/2)\varepsilon_{\text{m}}\text{Re}[f_{\text{CM}}]^2 r^2 E^2/(1 + h_{\text{m}}/r)^4$, where h_{m} is the surface to surface distance between the particle and the electrode.[26]

To further analyze the effect of these forces on particles' movement, the forces affecting on the AuNPs–PS hybrid particles in this optoelectrofluidic system were investigated [Fig. 3(a)]. The particles are initially focused to the upper side of the liquid chamber due to the vertical component of the dielectrophoretic force. The particles near the electrode surface are affected by the electrostatic particle–surface interaction force, being attracted toward the electrode surface.[12] While the ACEO flows originally occur toward the virtual electrode at the bottom of the liquid chamber, the converged fluids from the virtual electrode flow in the
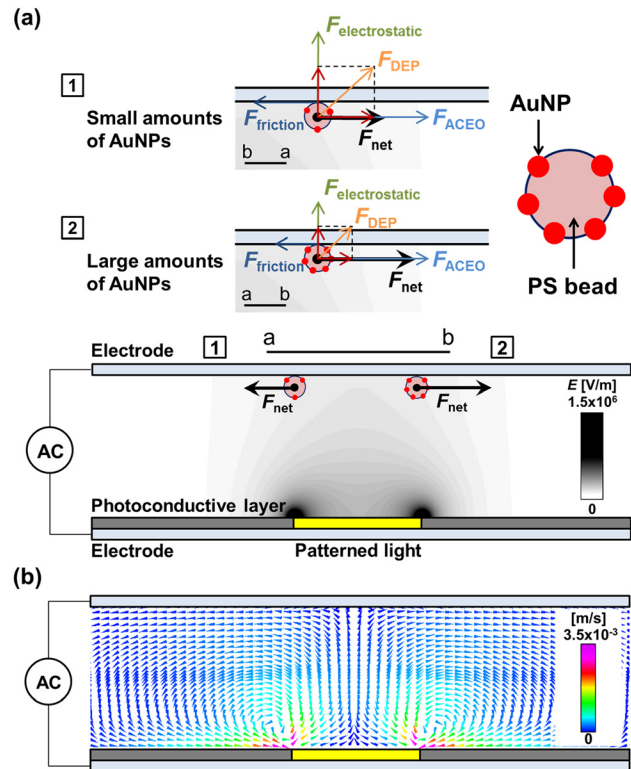

FIG. 3. (a) Force diagram on AuNPs–PS hybrid particles according to the amount of gold nanoparticles. Red arrows represent the vertical and the lateral components of the dielectrophoretic force. (b) Simulation of ACEO flow velocity distribution generated in the optoelectrofluidic system.

opposite direction at the top of the liquid chamber as shown in Fig. 3(b). As a result, the hydrodynamic drag force by the ACEO flows make the hybrid particle near the top electrode moved from the light pattern in a lateral direction. The DEP and the electrostatic particle–surface interaction forces depend on Re[f_{CM}], which is dependent on the amount of AuNPs on the PS particle. According to the scanning electron microscopic analysis (data not shown), the fraction of the gold-coated area in the hybrid particle surface was only 1% even after the immunoreaction with the highest antigen concentration. Thus we can expect that Re[f_{CM}] might still be less than 0 even though it was slightly shifted toward the positive in the AuNPs range we used [Fig. 2(b)]. With this little change in Re[f_{CM}], the sum of the vertical DEP force and the electrostatic surface–particle interaction force, which act as the normal force of the friction force, are weakened. As a consequence, the friction force cancelling the hydrodynamic drag force become weaker as the amount of AuNPs increased, resulting in the increase of the net force in the lateral direction. This behavior can be explained by our force balance model as follows:

$$F_{\text{ACEO}} + F_{\text{DEP\_lateral}} - k \cdot (F_{\text{DEP\_vertical}} + F_{\text{electrostatic}}) - F_{\text{drag}} = 0,$$

where F_{ACEO} is the hydrodynamic drag force due to the ACEO flow, $F_{\text{DEP\_lateral}}$ and $F_{\text{DEP\_vertical}}$ are the lateral and the vertical components of the dielectrophoretic force, respectively, $F_{\text{electrostatic}}$ is the electrostatic surface–particle interaction force, F_{drag} is the drag force, and k is the friction coefficient.
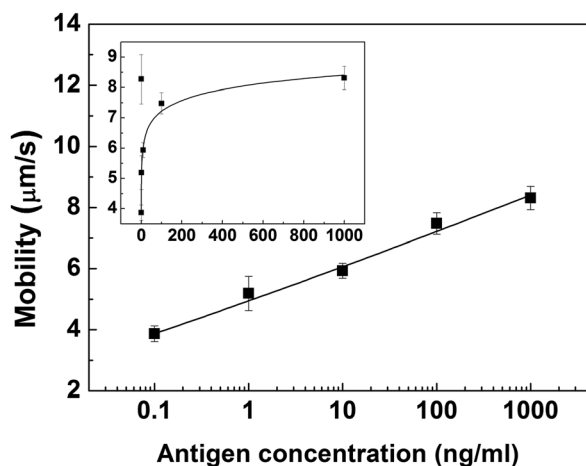
FIG. 4. Experimental results of mobility change of the AuNPs–PS hybrid particles according to the amount of analytes. The experimental data were fitted well to the force balance model that we hypothesized ($n = 15$, $R^2 = 0.983$). Both graphs have the same unit.

Fig. 4 shows the mobility change of the AuNPs–PS hybrid microparticles according to the amount of analytes (antigens) which are involved in the formation of AuNPs–PS immunocomplexes. The motility of AuNPs–PS hybrid particles increased as the amount of AuNPs on the PS particle increased; increasing antigen concentration implies that larger amounts of AuNPs are conjugated on the PS particle. The experimental results showed excellent agreement with the force balance model that we hypothesized. However, when no metal is conjugated on the PS particle, proper force balance condition for this model might be lost, resulting in exceptive disagreement as shown in zero concentration of the inset. This disagreement might be due to the other factors such as surface–particle interactions depending on the intrinsic properties of each material (i.e., hydrophobic interactions), which were not considered in our model.

Despite the lack of complete theoretical model applicable to all the experimental conditions, our study could provide significant impacts in the broad field from colloidal physics to immunochemistry. While the ACEO and the electrostatic forces acting on the microparticles, of which size is ranged from 4.5 to 150 μm, have been known to be negligible compared to the dielectrophoretic force at the relatively high ac frequency range in most cases,[2,3,14,27,28] our experimental investigation suggests that all the forces might significantly affect the particle behaviors and balance with each other. In addition, this study gave us a lesson that the slight differences in dielectric characteristics of the particles may result in the relatively large differences in behavior when such various force mechanisms act in concert. In this context, the mobility measurement based on optoelectrofluidic particle behaviors will be applicable to an optoelectrofluidic immunoassay, in which the small differences in the amount of antigens are detectable based on the difference in the particle velocity.

In this study, we presented that a variety of forces act on the behaviors of the particles in the optoelectrofluidic device in concert with each other. In particular, we discovered that not only the dielectrophoretic force but also other mechanisms such as the ACEO and the electrostatic interactions might also affect the movements of the metal–polymer hybrid particles in the application of ac voltage at a relatively high frequency around 100 kHz. From what we figure out, this result would present a perspective to understand the optoelectrofluidic particle dynamics as well as an analytical concept based on the optoelectrofluidic mobility of the immunocomplex microparticles, in which simple read-out platforms for quantifying the analyte concentration could be available. We anticipate that further investigations on the optoelectrofluidic particle behaviors and integration with other microfluidic systems would make progressive advances in a variety of fields of science and engineering.

[1]H. Hwang and J.-K. Park, Lab Chip **11**, 33 (2011).
[2]P. Y. Chiou, A. T. Ohta, and M. C. Wu, Nature (London) **436**, 370 (2005).
[3]H. Hwang, Y.-J. Choi, W. Choi, S.-H. Kim, J. Jang, and J.-K. Park, Electrophoresis **29**, 1203 (2008).
[4]H. Hwang, D.-H. Lee, W. Choi, and J.-K. Park, Biomicrofluidics **3**, 014103 (2009).
[5]A. T. Ohta, M. Garcia, J. K. Valley, L. Banie, H. Y. Hsu, A. Jamshidi, S. L. Neale, T. Lue, and M. C. Wu, Lab Chip **10**, 3213 (2010).
[6]W. Choi, S.-W. Nam, H. Hwang, S. Park, and J.-K. Park, Appl. Phys. Lett. **93**, 143901 (2008).
[7]H. Hwang and J.-K. Park, Anal. Chem. **81**, 5865 (2009).
[8]H. Hwang and J.-K. Park, Anal. Chem. **81**, 9163 (2009).
[9]H. Hwang, H. Chon, J. Choo, and J.-K. Park, Anal. Chem. **82**, 7603 (2010).
[10]H. Hwang, D. Han, Y. J. Oh, Y. K. Cho, K. H. Jeong, and J. K. Park, Lab Chip **11**, 2518 (2011).
[11]H. Hwang, J.-J. Kim, and J.-K. Park, J. Phys. Chem. B **112**, 9903 (2008).
[12]H. Hwang, Y. Oh, J.-J. Kim, W. Choi, J.-K. Park, S.-H. Kim, and J. Jang, Appl. Phys. Lett. **92**, 024108 (2008).
[13]H. Hwang, Y.-H. Park, and J.-K. Park, Langmuir **25**, 6010 (2009).
[14]J. K. Valley, A. Jamshidi, A. T. Ohta, H. Hsan-Yin, and M. C. Wu, J. Microelectromech. Syst. **17**, 342 (2008).
[15]Y. Jung, N. Singh, and K.-S. Choi, Angew. Chem. Int. Ed. **48**, 8331 (2009).
[16]J.-H. Lee, M. A. Mahmoud, V. Sitterle, J. Sitterle, and J. C. Meredith, J. Am. Chem. Soc. **131**, 5048 (2009).
[17]L. R. Hirsch, J. B. Jackson, A. Lee, N. J. Halas, and J. L. West, Anal. Chem. **75**, 2377 (2003).
[18]M. Han, X. Gao, J. Z. Su, and S. Nie, Nat. Biotechnol. **19**, 631 (2001).
[19]M. Schierhorn, S. J. Lee, S. W. Boettcher, G. D. Stucky, and M. Moskovits, Adv. Mater. **18**, 2829 (2006).
[20]Y.-J. Li, M. Xu, J.-Q. Feng, and Z.-M. Dang, Appl. Phys. Lett. **89**, 072902 (2006).
[21]G. T. Hermanson, *Bioconjugate Techniques* (Academic, New York, 1996), p. 173.
[22]L. Zhang and Y. Zhu, Appl. Phys. Lett. **96**, 141902 (2010).
[23]H. Morgan and N. G. Green, *AC Electrokinetics: Colloids and Nanoparticles* (Research Studies, 2003), p. 341.
[24]H. Hwang and J. K. Park, Lab Chip **9**, 199 (2009).
[25]See supplementary material at http://dx.doi.org/10.1063/1.4790622 for optically induced AC electroosmosis (ACEO) flow in the optoelectrofluidic device and Fig. S1.
[26]Z. Adamczyk, Adv. Colloid Interface Sci. **100–102**, 267 (2003).
[27]A. T. Ohta, Chiou Pei-Yu, H. L. Phan, S. W. Sherwood, J. M. Yang, A. N. K. Lau, H. Y. Hsu, A. Jamshidi, and M. C. Wu, IEEE J. Sel. Top. Quantum Electron. **13**, 235 (2007).
[28]Y.-H. Lin, Y.-W. Yang, Y.-D. Chen, S.-S. Wang, Y.-H. Chang, and M.-H. Wu, Lab Chip **12**, 1164 (2012).